

# Composition of chains in waxy-rice starch and its structural units

E. Bertoft<sup>a,\*</sup>, K. Koch<sup>b</sup>

<sup>a</sup>Department of Biochemistry and Pharmacy, Åbo Akademi University, BioCity, P.O. Box 66, FIN-20521 Turku, Finland

<sup>b</sup>Department of Food Science, Swedish University of Agricultural Sciences, P.O. Box 7051, S-750 07 Uppsala, Sweden

Received 19 March 1999; received in revised form 17 May 1999; accepted 17 May 1999

## Abstract

$\phi$ , $\beta$ -Limit dextrins of fractions of intermediate products obtained by alpha-amylolysis of waxy-rice starch were analysed for their unit chain distributions by gel-permeation chromatography. The proportion of long chains decreased in fractions of low-molecular-weight dextrins, but the ratio of A:B-chains, A:Ba-chains, and Ba:Bb-chains remained almost constant. High-performance anion exchange chromatography was used for a detailed analysis of the composition of B-chains. Chains with a length intermediate to the groups of short and long B-chains increased in small dextrins. The shortest B-chain in the  $\phi$ , $\beta$ -limit dextrins was maltotriose and was preferentially produced during alpha-amylolysis. Models are proposed showing the fine structure of the clusters of the amylopectin, that probably originated from different structural domains within the starch granules. © 2000 Elsevier Science Ltd. All rights reserved.

**Keywords:** Waxy-rice starch; Gel-permeation chromatography; Alpha-amylolysis

## 1. Introduction

Starch granules are organized into different structural levels. The first level includes the crystalline and amorphous “growth rings” (Yamaguchi, Kainuma & French, 1979). Recent studies with atomic force microscopy suggest that both of these structures are build up of units of blocklets (Baldwin, Adler, Davies & Melia, 1998; Gallant, Bouchet, & Baldwin, 1997). Ellipsoidal 400 nm particles of amylopectin were also observed inside the starch granules during gelatinization (Atkin, Abeysekera, Cheng & Robards, 1998). The molecular architecture of the amorphous ring is not known, but the existence of blocklets indicates a certain degree of organization in this area. In the crystalline blocklets the branched amylopectin component of the starch is organized into a second level of crystalline and amorphous lamellae (Gallant et al., 1997). The external, linear chains of the amylopectin exist as double helices in the crystalline lamellae, and the chains are connected through clustered  $\alpha$ -D-(1  $\rightarrow$  6)-branches mainly found within the amorphous lamellae (Imberty, Buléon, Tran & Pérez, 1991). In cereal starches, some branches are also scattered into the crystalline lamellae (Jane, Wong & McPherson, 1997).

Short unit chains of the amylopectin are arranged in clusters, whereas long chains interconnect the clusters

(Hizukuri, 1986). Long internal chain segments, like those found between the clusters, easily interact with the nine subsites of the alpha-amylase of *Bacillus amyloliquefaciens* (earlier referred to as the liquefying type of *B. subtilis*, Robyt & French, 1963). As a result a range of intermediate  $\alpha$ -dextrins are produced from which units of clusters can be isolated (Bertoft & Spoof, 1989; Zhu & Bertoft, 1996). In a previous work (Bertoft, Zhu, Andtfolk & Jungner, 1999), we isolated the intermediate dextrins, formed from waxy-rice starch (WRS, containing only amylopectin) by a 1 h and a 3 h alpha-amylolysis, into samples of different size-classes. Selected samples were treated successively with phosphorylase and beta-amylase to produce  $\phi$ , $\beta$ -limit dextrins ( $\phi$ , $\beta$ -LD) in which the external chains are reduced to maltosyl- and glucosyl-stubs (Bertoft, 1989).

Based on the pattern of a second alpha-amylolysis, we suggested that the  $\phi$ , $\beta$ -LD originated from structurally different domains, designated A and B (Bertoft et al., 1999). Whether these domains originated from different parts of the macromolecular amylopectin, or from the different types of crystalline and amorphous blocklets in the starch granule, is an open question.

Domain A possessed units of clusters with a degree of polymerization (d.p.) of 100–200, designated cIIIa, cIVa, and cVa in order of increasing size (Bertoft et al., 1999). By an extensive alpha-amylolysis, using 100  $\times$  more enzyme, the clusters were hydrolysed further into small dextrins representing branched building blocks of d.p. 5–40 (designated eII–eVI). Small amounts of linear dextrins with d.p.

\* Corresponding author. Tel.: + 358-2-265-4272; fax: + 358-2-265-4745.

2–4 (eI) were probably produced by a repetitive attack from internal chains inside the clusters. The size distribution profile of the building blocks, with comparatively high amounts of the larger building blocks eV and eVI, was characteristic for domain A. Domain B was characterized by clusters of less defined sizes with d.p. 90–130 (dextrins cIIb and cIVb) and a size-distribution of building blocks that became more narrow with decreasing d.p. and alpha-amylolysis time. In this work we have extended the research to a characterization of the types of chains found in the dextrin samples from domains A and B.

## 2. Experimental

### 2.1. Enzymes and samples

Isoamylase of *Pseudomonas amyloclavata* (glycogen 6-glucanohydrolase; EC 3.2.1.68) and pullulanase of *Klebsiella pneumoniae* (amylopectin 6-glucanohydrolase; EC 3.2.1.41) were obtained from Hayashibara Shoji Inc. According to the supplier, the activity of the isoamylase was 71 000 U/mg (1 mg/ml), in which the unit was based on the increase of the absorbance of a starch solution stained with iodine according to Yokobayashi, Misaka and Harada (1970), whereas the activity of the pullulanase was 40.4 U/mg (10 mg/ml), 1 U catalyzing the liberation of 1  $\mu$ mol of maltotriose/min from pullulan at pH 6.0 and 30°C. Beta-amylase from sweet potato [(1  $\rightarrow$  4)- $\alpha$ -D-glucan maltohydrolase; EC 3.2.1.2] was from Sigma and had an activity given by the supplier of 880 U/mg (26 mg/ml), 1 U catalyzing the liberation of 1 mg of maltose in 3 min from starch at pH 4.8 and 20°C. The waxy-rice starch and the samples of  $\phi$ , $\beta$ -LD of the WRS and of  $\alpha$ -dextrins obtained after 1 and 3 h of hydrolysis were identical to those described by Bertoft et al. (1999).

### 2.2. Complete debranching

WRS and the  $\phi$ , $\beta$ -LD of WRS (3.6 mg) were dissolved in 90% DMSO (0.5 ml) in a boiling water bath for 15 min with subsequent stirring for 48 h at room temperature. The WRS sample was diluted with 0.06 M NaOAc buffer (2.5 ml, pH 3.6) before undiluted isoamylase (5  $\mu$ l) was added. The sample was debranched overnight in a shaking water-bath at 38°C, boiled, and analysed by HPAEC-PAD as described below.

The  $\phi$ , $\beta$ -LD of WRS was diluted with 0.1 M NaOAc buffer (2.5 ml, pH 5.5) before addition of pullulanase (5  $\mu$ l). The  $\phi$ , $\beta$ -LD of the hydrolysis products obtained after alpha-amylolysis of WRS (Bertoft et al., 1999) were dissolved in water (2.4 mg in 0.75 ml) on a boiling water-bath for 5–10 min before addition of NaOAc buffer (0.075 ml) and pullulanase (5  $\mu$ l). The samples were debranched overnight at room temperature and boiled.

### 2.3. Partial debranching of $\phi$ , $\beta$ -LD and beta-amylolysis

Partial debranching with a diluted isoamylase solution was performed as described by Zhu and Bertoft (1996), but with slight modifications because it was difficult to obtain reproducible dilutions of the enzyme. Instead, the enzyme suspension obtained from the supplier was centrifuged and the supernatant, which contained a low enzyme activity, was diluted twice with 0.1 M NaOAc buffer, pH 3.5. This solution was estimated to contain  $\sim$ 100 U/ml when comparing the time to achieve complete hydrolysis of WRS with the non-diluted enzyme. With the diluted enzyme the partial debranching was empirically tested (Zhu & Bertoft, 1996) to be completed within 4 h, when a sample of  $\phi$ , $\beta$ -LD in water (3 mg in 1.5 ml) was treated with the enzyme solution (95  $\mu$ l,  $\sim$ 10 U) at 25°C. The reaction was stopped by boiling for 10 min and an aliquot (0.2 ml) was used for gel-permeation chromatography. Another aliquot (0.45 ml) was diluted with 0.1 M NaOAc buffer (0.15 ml, pH 4.8) and incubated with beta-amylase (2.5  $\mu$ l) overnight at room temperature before gel-permeation chromatography.

### 2.4. Gel-permeation chromatography

Aliquots (0.2 ml) of the debranched samples ( $\sim$ 1.2 mg/ml) in 0.5 M KOH were applied on columns (1.0  $\times$  90 cm<sup>2</sup>) of Superdex 30 or Superdex 75 (Pharmacia) and eluted with 0.5 M KOH at 0.5 ml/min. Fractions (0.5 ml) were analysed for carbohydrates with the phenol-H<sub>2</sub>SO<sub>4</sub> reagent (Dubois, Gilles, Hamilton, Rebers & Smith, 1956). The columns were calibrated as described earlier (Bertoft, 1991a; Bertoft & Spoof, 1989).

### 2.5. High-performance anion-exchange chromatography (HPAEC-PAD)

The chromatography was performed on a Dionex DX 500 instrument (Sunnyvale, CA, USA) equipped with a pulsed amperometric detector (ED 40) essentially according to (Koch, Andersson & Åman, 1998). Debranched samples (0.2–0.7 mg/ml) were filtered and an aliquot (20  $\mu$ l) was injected onto a CarboPac PA-100 anion exchange column (250  $\times$  4 mm<sup>2</sup>) in combination with a CarboPac PA-100 guard column. The acetate gradient system included two eluents: eluent A was 150 mM NaOH and eluent B was 150 mM NaOH containing 500 mM NaOAc. The system was equilibrated with the initial eluent mixture at 1 ml/min for 15 min before each run. The elution gradient was: 0–5 min, linear gradient from 34.3 to 45% eluent B; 5–55 min, linear gradient to 67% eluent B; and 55–80 min, linear gradient to 90% eluent B.

Table 1

Characteristics of  $\phi$ , $\beta$ -LD obtained after alpha-amylolysis of waxy-rice amylopectin (from Bertoft et al., 1999)

Sample <sup>a</sup>	Alpha-amylolysis (h)	Type of structure <sup>b</sup>	D.p.	Number of blocks <sup>c</sup>	Density of blocks <sup>d</sup>
Amylopectin	0	Mixed	—	—	—
2.1	1	DomA	272	14.5	5.3
10.1	3	DomA	110	5.8	5.3
10.2	3	DomA	75	4.1	5.5
7.2.1 <sup>c</sup>	1	DomB(?)	176	—	—
7.2.2	1	DomB	139	8.4	6.1
3	1	DomB	66	4.2	6.4
11.1	3	DomB	47	3.1	6.7
11.2	3	DomB	34	2.3	6.7
13	3	DomB(?)	16	1.2	7.7

<sup>a</sup> The hydrolysis mixtures were fractionated by methanol and the precipitates were numbered successively. Re-fractionated samples were given additional successive numbers (e.g. samples 10.1 and 10.2 were sub-fractions of sample 10, etc.).

<sup>b</sup> Referred to as domain A and B by Bertoft et al. (1999).

<sup>c</sup> Average number of branched blocks eII–eVI in the dextrans.

<sup>d</sup> (Number of blocks)/(d.p. of fraction)  $\times$  100.

<sup>e</sup> Not reported earlier.

### 3. Results

#### 3.1. Composition of different types of chains in $\phi$ , $\beta$ -LD

The series of fractions of  $\phi$ , $\beta$ -LD from WRS was isolated and partly characterized earlier (Bertoft et al., 1999). Some of their characteristics are summarized in Table 1. The fractions were produced by two large batches of alpha-amylolysis for 1 and 3 h and grouped into two types of structures possibly originating from different domains, here designated DomA and DomB (to avoid confusion with A- and B-chains or with A- and B-type starches). Sample 7.2.1 was not included in our earlier investigation, but most probably it possessed a structure of type DomB, because it was a sub-fraction of sample 7.2, to which also 7.2.2 belonged. The average d.p. of the fractions ranged from 16 to 272.

Small sub-cluster dextrans were obtained by an extensive alpha-amylolysis and were regarded as units of building blocks that build up the units of clusters in the amylopectin

(Bertoft et al., 1999). The average number of branched blocks in the fractions ranged from 1.2 to 14.5 (Table 1). The density of the branched building blocks was also defined earlier and it was found to be somewhat higher in DomB-type dextrans than in those of DomA.

The fractions were submitted to complete debranching with pullulanase and the unit chain profiles were analysed by gel-permeation chromatography on Superdex 30 and on Superdex 75 (Fig. 1(a) and (b)). The B-chains (chains substituted by other chains, Peat, Whelan & Thomas, 1952) of the  $\phi$ , $\beta$ -LD of WRS could be divided into two groups of long and short chains with d.p.  $\geq 23$  and  $< 23$ , respectively (Fig. 1(b)). On the Superdex 30 column the longer chains were eluted at the void volume (Fig. 1(a)). As a result of the attack by the alpha-amylase, the long B-chains were reduced in length and number, and the ratio of short:long chains increased both with the incubation time and with the decrease of dextrin size (Table 2). The A-chains (unsubstituted chains, Peat et al., 1952) were

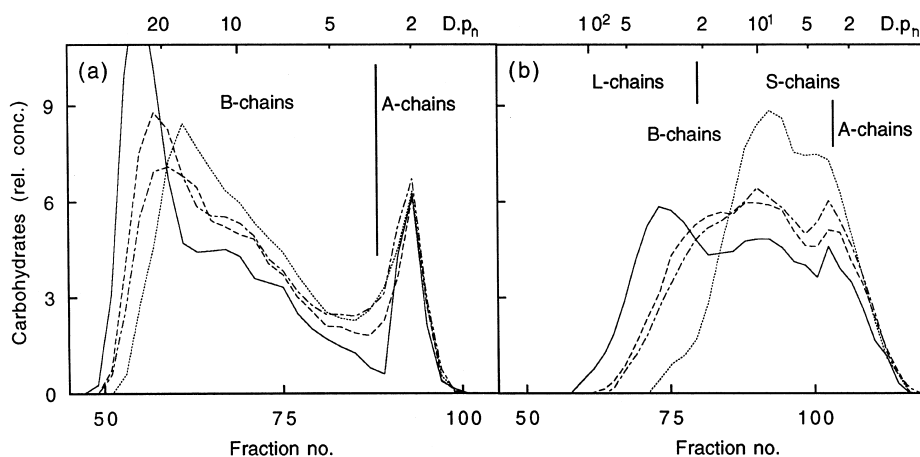


Fig. 1. Distribution on (a) Superdex 30 and (b) Superdex 75 of the unit chains of completely debranched  $\phi$ , $\beta$ -LD of WRS (—) and samples 3 (---), 10.2 (-.-), and 11.2 (···). The ranges of A- and B-chains and of short (S) and long (L) chains are shown.

Table 2

Chain ratios in fractions of  $\phi$ , $\beta$ -LD obtained from gel permeation chromatography on Superdex 75

Sample	S:L <sup>a</sup>	A:B	A:B	Ba:Bb
Amylopectin	10.5:1	0.8:1	1.2:1	1.8:1
2.1	15.7:1	0.9:1	1.4:1	2.0:1
10.1	23.2:1	0.9:1	1.4:1	1.9:1
10.2	23.9:1	0.9:1	1.4:1	2.0:1
7.2.1	14.5:1	0.7:1	1.2:1	1.8:1
7.2.2	15.6:1	0.8:1	N.a. <sup>b</sup>	N.a.
3	18.9:1	0.9:1	1.4:1	2.1:1
11.1	24.9:1	0.8:1	1.2:1	1.9:1
11.2	36.0:1	0.9:1	1.4:1	1.9:1
13	109.3:1	0.8:1	1.2:1	1.7:1

<sup>a</sup> Ratio of short chains (c.l. < 23) to long chains (c.l.  $\geq$  23).

<sup>b</sup> Not analysed.

represented by the maltose peak, which was poorly resolved in the chromatograms obtained from the column of Superdex 75. Therefore, the results from Superdex 30 were used for a quantitative estimation of the maltose in the samples, whereas the distribution of B-chains was obtained from Superdex 75 (Fig. 1(a) and (b), respectively). The molar ratio of A:B-chains was 0.8:1 in the amylopectin and was similar in all the fractions obtained after the alpha-amylase attack (Table 2).

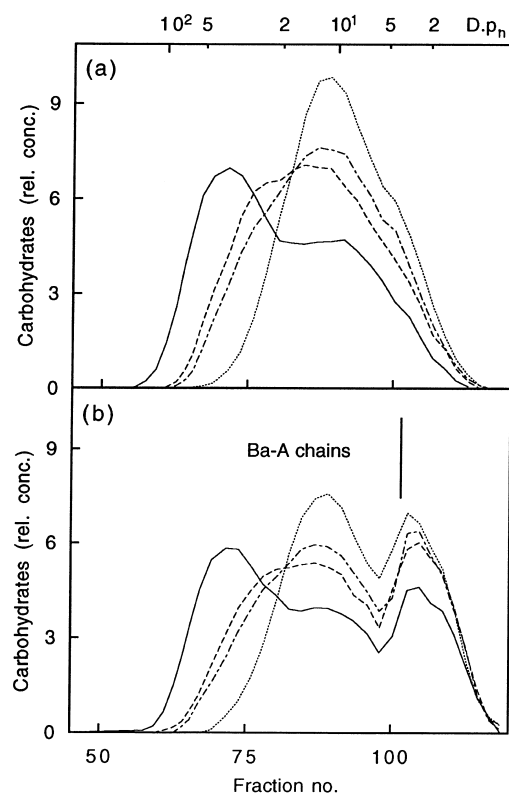


Fig. 2. Distribution on Superdex 75 of (a) Ba-A- and Bb-chains after partial debranching and (b) the Ba-A-chains after a successive beta-amylolysis of the  $\phi$ , $\beta$ -LD of WRS (—) and samples 3 (---), 10.2 (-.-), and 11.2 (···). The range of Ba-A-chains is shown.

$\phi$ , $\beta$ -LD can be used for the estimation of Ba-chains (Zhu & Bertoft, 1996), which are defined as chains substituted with at least one A-chain, whereas those only substituted with other B-chains are called Bb-chains (Hizukuri & Maehara, 1990). The affinity of isoamylase for a short branch with only a maltosyl chain-stub is very low compared to longer branches. A partial debranching with the isoamylase leads under suitable conditions to an attack at all branches except at those carrying the maltosyl stubs (Hizukuri & Maehara, 1990). When submitted to such partial debranching, the profiles of the linear Bb-chains and the branched Ba-chains carrying the A-chain stubs (Ba-A chains) also possessed the two types of short and long chains (Fig. 2(a)). After treatment with beta-amylase, the Bb-chains were hydrolysed into maltose and, as for the completely debranched samples, the peak for maltose was mixed with other very small dextrans (Fig. 2(b)). The residual profile showed the distribution of the Ba-A chains, which was similar to that after the partial debranching and suggested that both Ba- and Bb-chains were found in all chain categories. The molar amount of Ba-chains was calculated from the chromatogram in Fig. 2(b) and the amount of Bb-chains was estimated as the difference between all B-chains and the Ba-chains (Hizukuri & Maehara, 1990). The ratio of A:Ba-chains was 1.2:1 in the amylopectin. Samples 2.1–10.2, that contained DomA-type structures, had a slightly higher ratio of 1.4:1 and in the fractions with DomB-type structures the ratio shifted slightly between 1.2:1 and 1.4:1. The ratio of Ba:Bb-chains ranged from 1.7:1 to 2.1:1. These small differences were, however, within experimental error.

The completely debranched samples were also used for the estimation of the average chain lengths (c.l.), which in the amylopectin  $\phi$ , $\beta$ -LD was 8.2 (Table 3). In the limit dextrans of the isolated fractions the c.l. was reduced as a function of the time of alpha-amylolysis and the size of the dextrans. Sample 2.1, which had the largest d.p. and contained DomA-type dextrans from the 1 h hydrolysis mixture, had a c.l. of 7.1. At 3 h the c.l. of the DomA-type dextrans was reduced to  $\sim$ 6.5 (samples 10.1 and 10.2). DomB-type dextrans possessed comparatively large values. Sample 7.2.1, with a d.p. less than sample 2.1, had a slightly longer c.l. value of 7.6, and the same trend was found for the other samples in this group.

The average number of chains (n.c.) ranged from 2.8 in sample 13 to 38.5 in sample 2.1 (Table 3). The number of branches (n.b.) is one less than the n.c. and the density of branches was expressed as (n.b.)/(d.p.)  $\times$  100. The density of the branches was somewhat higher in DomA dextrans (13.8–14.5) than in the series of DomB dextrans ( $\sim$ 13). The lowest density of 11.3 was found in the small dextrans of sample 13 that on average had approximately two branches. From the number of branched building blocks (Table 1), the average number of branches within the building blocks was estimated as (n.b.)/(number of blocks). As shown in Table 3, the n.b. per block in the DomA-type

Table 3

Chain length and density of branches in fractions of  $\phi$ , $\beta$ -LD obtained from waxy-rice amylopectin

Sample	C.l. <sup>a</sup>	N.c. <sup>b</sup>	N.b. <sup>c</sup>	Density of branches <sup>d</sup>	N.b. per block <sup>e</sup>
Amylopectin	8.2	—	—	—	—
2.1	7.1	38.5	37.5	13.8	2.6
10.1	6.5	17.0	16.0	14.5	2.8
10.2	6.4	11.8	10.8	14.4	2.6
7.2.1	7.6	23.3	22.3	12.7	—
7.2.2	7.3	19.0	18.0	13.0	2.1
3	6.8	9.8	8.8	13.3	2.1
11.1	6.7	7.0	6.0	12.8	1.9
11.2	6.2	5.5	4.5	13.2	2.0
13	5.7	2.8	1.8	11.3	1.5

<sup>a</sup> Chain length obtained by gel permeation chromatography on Superdex 75.<sup>b</sup> Number of chains = d.p./c.l.<sup>c</sup> Number of branches = n.c. – 1.<sup>d</sup> (N.b.)/(d.p.)  $\times$  100.<sup>e</sup> Average number of branches in building blocks.

dextrins was typically higher ( $\sim 2.6$ ) than in DomB dextrins ( $\sim 2.0$ ) and was apparently independent of the size of the dextrins within each structural type. Sample 13, classified as a DomB-type structure was somewhat uncertain (Bertoft et al., 1999), had only 1.5 branches per block.

### 3.2. Distribution of B-chains

The distribution of chains in the original WRS, obtained by complete debranching with isoamylase, was compared with that of its  $\phi$ , $\beta$ -LD by analysis with HPAEC-PAD (Fig. 3(a) and (b)). The group of short chains of the WRS possessed a maximum at d.p. 12 and a shoulder at d.p. 18–20, in accordance with a recent report (Hanashiro, Abe & Hizukuri, 1996). The long chains had a maximum at d.p. 43 and the longest chains that could be detected had a d.p. of 62. Though the chromatogram possessed a minimum at d.p. 38, a clear division between the groups of chains could not be done. On the basis of the composition of the chains of the  $\phi$ , $\beta$ -LD, in which the long chains had d.p.  $\geq 23$ , and the external chain length (e.c.l) of the WRS (which was 11), the long chains of the WRS would be expected to have a d.p. of approximately  $\geq 33$  (Fig. 3(a)).

The amount of maltose released from the  $\phi$ , $\beta$ -LD upon debranching was very large compared to the other chain lengths. In addition, the maltose gives the highest response by pulsed amperometric detection (Koch et al., 1998). These circumstances made it very difficult to get a correct quantitative estimation of the maltose simultaneously with the longer chains within the same sample. For this reason the results from HPAEC-PAD were only used for the detailed study of the composition of the B-chains in the samples of  $\phi$ , $\beta$ -LD. The B-chains of the WRS  $\phi$ , $\beta$ -LD were clearly divided into long and short at d.p. 23 (Fig. 3(b)). The profile of the short B-chains suggested a further sub-division. Based on the nomenclature used in an earlier study on  $\phi$ -LD of waxy-maize starch (Bertoft, 1991b), B1a-chains were defined as chains with d.p.  $< 14$ , and B1b-chains had d.p. 14–22. The details in the chromatograms suggested, however, a further sub-division of the B1a-chains into longer chains [B1a(1)] with d.p. 8–13 and shorter chains [B1a(s)] with d.p. 5–7. The shortest B-chains with d.p. 3

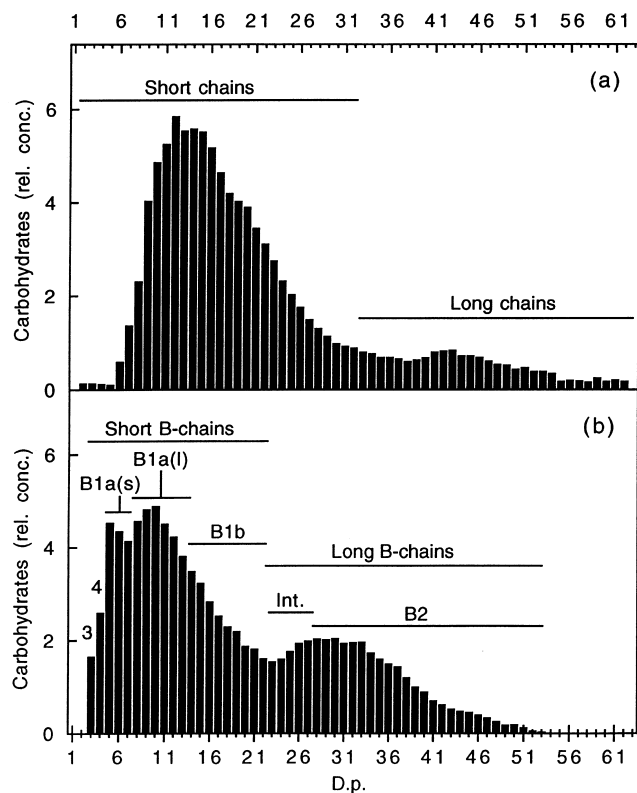


Fig. 3. Bar graphs showing the chain length distribution on HPAEC-PAD of (a) WRS and (b) the B-chains of the  $\phi$ , $\beta$ -LD of WRS. Groups of different chains and of maltotriose (3) and maltotetraose (4) are shown.

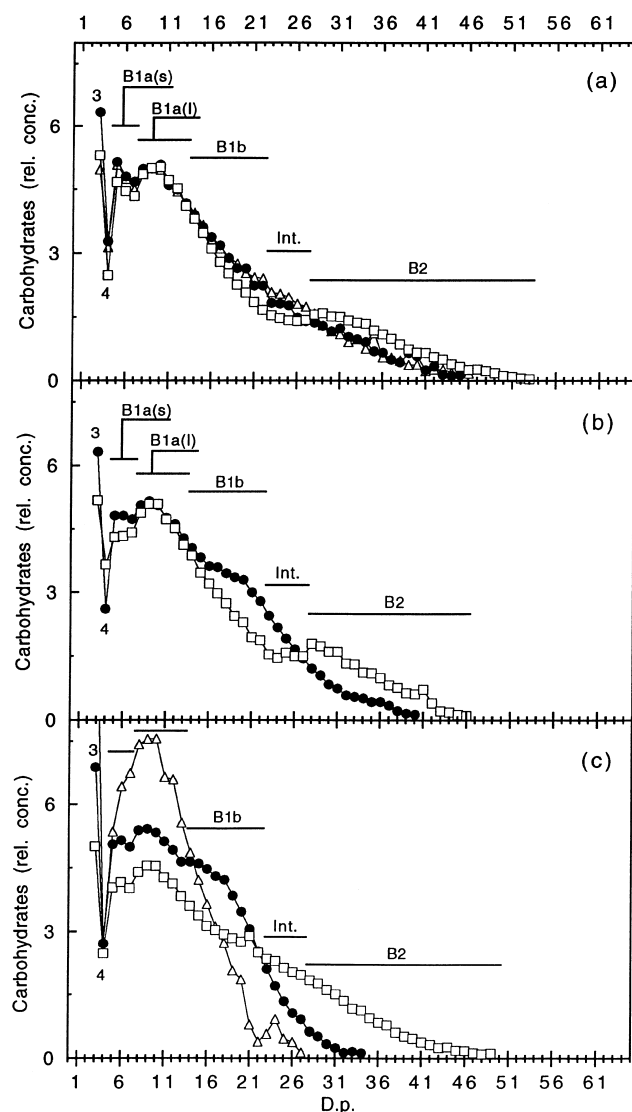


Fig. 4. Distribution of B-chains on HPAEC-PAD of the  $\phi,\beta$ -LD of: (a) samples 2.1 ( $\square$ ), 10.1 ( $\bullet$ ), and 10.2 ( $\triangle$ ); (b) samples 7.2.1 ( $\square$ ) and 11.1 ( $\bullet$ ); and (c) samples 3 ( $\square$ ), 11.2 ( $\bullet$ ), and 13 ( $\triangle$ ). Groups of different chains and of maltotriose (3) and maltotetraose (4) are shown.

and 4 were found in comparatively low amounts and were therefore not considered as B1a(s)-chains.

For reasons discussed below, the long B-chains were also subdivided. B2-chains had d.p. 28–53 and a narrow group with d.p. 23–27 was designated as intermediate chains (Fig. 3(b)). This group of chains was similar to a group called B1c that was earlier found in the  $\phi$ -LD of waxy-maize starch, though in that sample they were classified as a sub-group of the short chains (Bertoft, 1991b).

The composition of B-chains was also analysed in the fractions of  $\phi,\beta$ -LD obtained after alpha-amylolysis. The distributions of the samples possessing DomA-type structure are shown in Fig. 4(a). Sample 2.1, obtained after 1 h of alpha-amylolysis, still contained the longest B2-chains, though the amount of this group of chains had been reduced

when compared to the original  $\phi,\beta$ -LD of WRS. The amount of intermediate chains had also decreased somewhat, whereas that of the short chains was practically unchanged. The exception was maltotriose that had increased more than three times and now both on a total carbohydrate and on a molar basis represented the most common single species of the B-chains. After an additional 2 h of hydrolysis the amount of B2-chains had decreased somewhat more (samples 10.1 and 10.2). Instead a small increase of the intermediate and B1b-chains was found together with the shorter B1a-chains. The B1a(l)-chains remained at a constant relative amount.

The B-chain distributions of dextrans of the DomB-type structure are shown in Fig. 4(b) and (c). Larger dextrans of the size found in sample 7.2.1 were earlier shown to be preferentially hydrolysed into those found in sample 11.1 (Bertoft et al., 1999). These two samples are compared in Fig. 4(b). Sample 7.2.1 had a very similar distribution of B-chains as sample 2.1, but the additional 2 h of hydrolysis resulted in a more profound attack on the B2-chains and a clear increase of intermediate and B1b-chains. A small increase of B1a(s)-chains (and of maltotriose) was also found, whereas again B1a(l)-chains remained unchanged. Sample 3, that represented smaller dextrans obtained in the 1 h hydrolysis mixture, possessed a similar composition of B2-chains as the larger dextrans in sample 7.2.1, but increased amounts of the intermediate chains and of longer B1b (Fig. 4(c)). The chains within the group of B1a were all found in somewhat lower amounts. Dextrans of the sizes found in sample 3 were preferentially hydrolysed into sizes represented in sample 11.2 (Bertoft et al., 1999). In this sample all long B-chains had decreased in amounts and all short chains (especially B1b) had increased. Sample 13, containing the smallest dextrans in the 3 h alpha-amylolysis mixture, possessed mostly increased relative amounts of the B1a-chains, with the exception of maltotetraose. Only remnants of intermediate chains remained.

## 4. Discussion

### 4.1. Characterization of unit chains in WRS

In our earlier study of the dextrans obtained by an extensive alpha-amylolysis, it was found that the  $\phi,\beta$ -LD of WRS had a different composition to that of the intermediate dextrans isolated from it (Bertoft et al., 1999). The WRS  $\phi,\beta$ -LD possessed more small building blocks than the fractions of DomA and DomB dextrans. Therefore, the unit chain profile of the WRS and its  $\phi,\beta$ -LD represented a mixture of chains from different structural parts (or domains) found within the starch granule or within the amylopectin macromolecule.

It was suggested that the A-chains in amylopectins in general are the shortest chains within the fraction of short chains (Hanashiro et al., 1996; Inouchi, Glover & Fuwa,

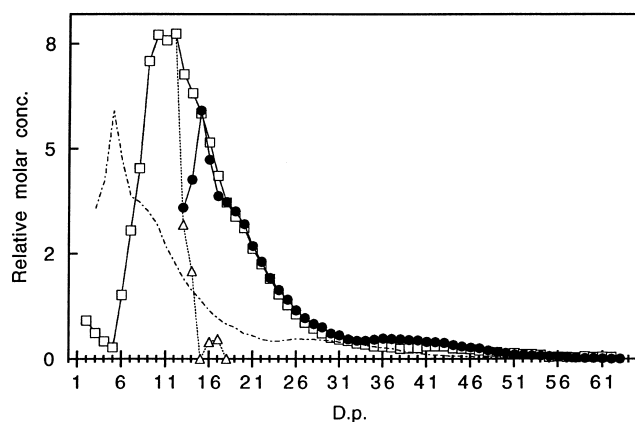


Fig. 5. Molar distribution of unit chains on HPAEC-PAD of WRS (□), and the B-chains of its  $\phi,\beta$ -LD (---). The distribution of the chains of the  $\phi,\beta$ -LD is superimposed (●) on the profile of WRS and the A-chains in WRS are theoretically traced as the difference between the two curves (△).

1987; Ong, Jumel, Tokarczuk, Blanshard & Harding, 1994), and based on this assumption the ratio of A:B-chains for waxy-rice amylopectin was estimated to 1.8–2.2 (Hizukuri, 1986; Ong et al., 1994). The reported values based on the estimation of maltose and maltotriose as A-chains in WRS  $\beta$ -LD are in the range 1.2–1.5 (Asaoka, Okuno & Fuwa, 1985; Enevoldsen & Juliano, 1988; Yun & Matheson, 1993). In comparison, the ratios obtained with the former method tend to be high. The ratio of A:B-chains in this work (Table 2) was low when compared with the reported values. We used the  $\phi,\beta$ -LD of WRS, in which all A-chains are found as maltose, and the shortest possible B-chain is maltotriose (Bertoft, 1989). This is in contrast with the  $\beta$ -LD, in which also some B-chains can appear as maltotriose (Yun & Matheson, 1993) and, thus, cause an overestimation of the amount of A-chains (and an underestimation of B-chains).

As seen in Fig. 3(a), it was practically impossible to make a distinction between A-chains and the short B-chains in WRS in accordance with the suggestion that all A-chains are the shortest ones in the amylopectin. It was therefore of interest to try to trace the A-chains within the profile of WRS. In the  $\phi,\beta$ -LD, the external segments of the B-chains have been reduced into one D-glucosyl residue (Bertoft, 1989), thereby causing a shortening of the original chains. If it is assumed that all B-chains had the same e.c.l. (Inouchi et al., 1987), and that this equalled the average e.c.l. in the amylopectin, which was 11, then all B-chains should have been reduced by 10 residues. The molar amount of chains should, however, still remain the same as in the original WRS, and therefore it would be possible to superimpose the molar distribution of the B-chains of the  $\phi,\beta$ -LD onto the B-chains of the WRS. Because the ratio of A:B-chains was 0.8 (Table 1), the B-chains represented 55% of all chains in the amylopectin. This factor was used to obtain an estimation of the relative molar concentration of the B-chains in the  $\phi,\beta$ -LD in Fig. 3(b) (in which the A-chain concentration was uncertain) comparable to that of WRS.

In Fig. 5 the molar concentrations of chains in WRS is compared to the concentration of B-chains in the  $\phi,\beta$ -LD after adding a d.p. of 10 to each chain type. The two curves fitted almost perfectly in the d.p. range 18–32. Interestingly, this part of the profile included the groups of B1a(l)- and B1b-chains and would suggest not only that no A-chains existed of similar lengths, but also that each chain of this type had an external length that closely corresponded to the experimental average. At low d.p. the reconstructed superimposed curves suggested that only A-chains existed, whereas at d.p. 13 and 14 the difference between the two curves represented the amount of A-chains, and thus there was a mixture of the two types of chains. The d.p. range 15–17 represented B1a(s)-chains. Except for d.p. 15, the result suggested very small amounts of A-chains within this size-class. Finally, the situation was different within the region corresponding to long chains, in which the molar concentration of chains with d.p. 33–47 was slightly higher in the reconstructed  $\phi,\beta$ -LD than in the WRS. Perhaps the longest chains preferentially had e.c.l. values >11, but a common internal length in the range 23–37, and therefore could not be superimposed on the WRS chain profile. Indeed, the average length of the apparent A-chains in the reconstruction was 10, so when the average e.c.l. was 11, some of the B-chains should possess longer external segments.

#### 4.2. Composition of chains in samples of $\phi,\beta$ -LD

The ratio of A:B-chains in the samples of  $\phi,\beta$ -LD obtained from the WRS was almost similar to the original sample. This suggested that both A- and B-chains were produced as a result of the alpha-amylase attack at the internal chains, with no special preference. The result was similar to that obtained earlier for waxy-maize starch, in which all dextrans possessed the same ratio of 1:1 as in the amylopectin (Bertoft, 1991b). In a potato amylopectin, however, the ratio increased with decreasing size of the dextrans from 1.4:1 to 1.8:1 (Zhu & Bertoft, 1996). This suggested fundamental differences in the predominating mode of interconnection of structural units within the amylopectins of the tuber and the cereal starches.

The amount of A-chains was best obtained by gel-permeation chromatography on Superdex 30, whereas the short B-chains strongly interfered with the maltose peak when Superdex 75 was used (Fig. 1). This was also the case after the partial debranching and the successive  $\beta$ -amylolysis to obtain the profile of Ba-A-chains (Fig. 2(b)), which made the estimation of the amount of Ba-chains uncertain. The ratios of A:Ba and Ba:Bb (Table 2) are therefore approximations. However, compared to potato amylopectin, the ratios were lower (Zhu & Bertoft, 1996). In the potato sample the ratios were also clearly dependent on the size of the dextrans, whereas for the WRS the ratios were more or less unaffected by both the size of the dextrans and the time of the alpha-amylolysis. Again, this suggested differences in the architecture of the two amylopectins. In

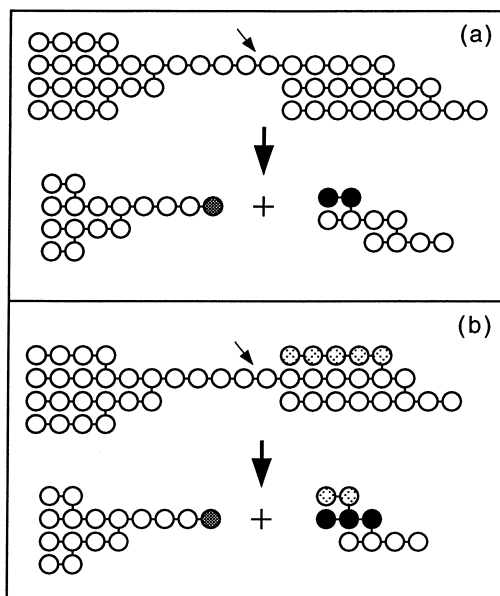


Fig. 6. Schematic presentation of the preferred mode of binding of structural branched units in the amylopectin of WRS: (a)  $\alpha$ -amylase attacks a long internal chain segment (arrow) on a B-chain. After treatment of the residual  $\alpha$ -dextrins with phosphorylase and beta-amylase to produce their  $\phi,\beta$ -LD, the dextrin to the right possesses its new A-chain as a maltosyl residue. The other segment of the B-chain (carrying a new reducing end-group) on the dextrin to the left will have a length corresponding to the intermediate or the B1b-chains; (b) the  $\alpha$ -amylase attacks a B-chain that on the fragment to the right possess a configuration of the Haworth type with two directly adjacent branches, which in the  $\phi,\beta$ -LD appears as a maltotriosyl residue. There is no other branch between the maltotriosyl fragment and the position of the attack: the circles represent glucosyl residues, black circles the maltosyl and maltotriosyl residue, dotted circles can be residues in either A- or B-chains, and the new reducing end formed after  $\alpha$ -amylase attack is gray.

addition, the maltose peak obtained from debranched  $\phi,\beta$ -LD of the potato amylopectin and its  $\alpha$ -dextrins was much better separated by Superdex 75, suggesting differences in the detailed composition of the shortest B-chains.

It was not possible to divide the samples into the two major types of DomA and DomB dextrans only on the basis of the chain length distributions. However, details in the composition of the B-chains obtained by HPAEC-PAD showed preferential patterns of the B1a(s)-chains. The samples containing dextrans of the DomA-type possessed a maximum at d.p. 5 (Fig. 4(a)), which was similar to the amylopectin  $\phi,\beta$ -LD (Fig. 3(b)). DomB-type dextrans possessed almost equal weight average amounts of all their B1a(s)-chains (Fig. 4(b) and (c)). Though small, this detail could indicate principal differences within the cluster structures.

When  $\alpha$ -amylase attacks an internal chain (e.g. between two clusters) a new external chain will be produced on one of the new fragments. As already discussed, this chain was either an A- or a B-chain. The HPAEC-PAD analyses showed that the preferred type of B-chain produced was of a type that became maltotriose after further reduction

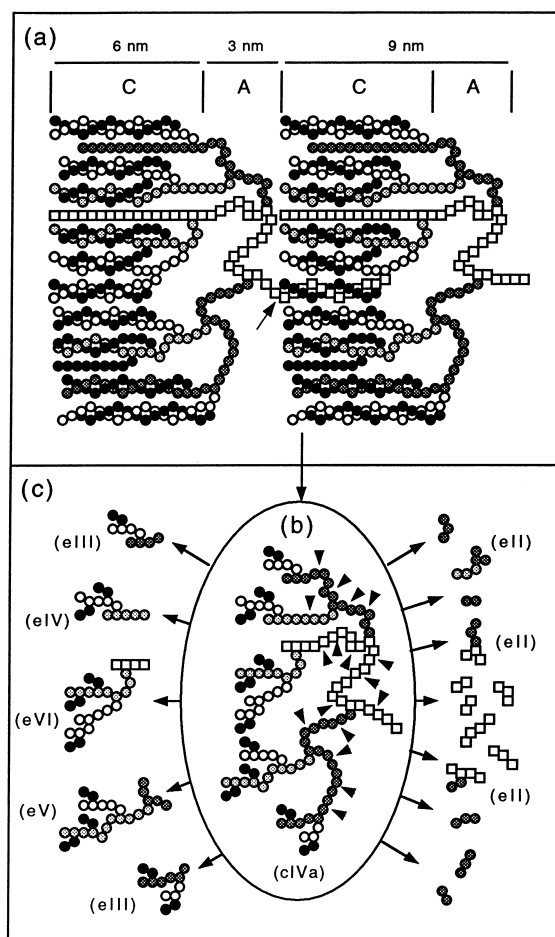


Fig. 7. Proposed model of the structure of domain A (DomA): (a) two clusters within a crystalline "growth ring" occupy the crystalline and amorphous lamellae (C and A, respectively) and the long internal chain segment is attacked at initial stages of  $\alpha$ -amylolysis (arrow); (b) the attack results in free clusters that were isolated as  $\phi,\beta$ -LD, represented here by dextrin cIVa. An extensive  $\alpha$ -amylolysis attacks the internal chain segments within the amorphous lamellae (small arrows); (c) branched building blocks of characteristic sizes (eII–eVI) are released together with very short linear maltodextrans: black circles represent A-chains, white circles B1a(s)-chains, light gray circles B1a(l)-chains, dark gray circles B1b-chains, and squares long chains (intermediate and B2-chains).

of the new external segment into a D-glucosyl residue by phosphorylase and beta-amylase. These two preferred attack patterns are shown in Fig. 6. The configuration giving rise to the maltotriose is of the Haworth type with two directly adjacent branches, which was shown to be common in waxy-rice amylopectin (Umeki & Yamamoto, 1975). The result was interesting, because it also showed the preferred mode of interconnection between structural units, and thus also indicated a preferred mode of biosynthesis of the amylopectin.

The other part of the attacked chain carries a new reducing end (Fig. 6). Probably, these types of chains were found as the intermediate and the B1b-types, which increased after longer times of  $\alpha$ -amylolysis, especially in the DomB dextrans (Fig. 4). If the B1a(s)-chains also represented this



Table 4  
Parameters of proposed structures of  $\phi$ , $\beta$ -LD

Parameter	cIVa		cIVb		cIb	
	Theor. <sup>a</sup>	Exp. <sup>a</sup>	Theor.	Exp.	Theor.	Exp.
D.p.	137	150	96	130	39	45
N.c. <sup>b</sup>	23	23	16	17	7	8
C.I. <sup>c</sup>	6.0	6.5	6.0	7.3	5.6	6.2
No. of building blocks <sup>d</sup>						
Total	18	17.8	17	19.1	7	7.1
EvI	1	1.0	–	0.6	–	0.2
eV	1	0.9	1	0.8	–	0.3
eIV	1	1.3	1	1.3	1	0.5
eIII	2	2.0	2	2.1	1	0.9
eII	3	2.7	3	3.0	1	1.1
eI (linear)	10	9.9	10	11.3	4	4.1
el:branched blocks <sup>d,e</sup>	1.25:1	1.25:1	1.43:1	1.45:1	1.33:1	1.37:1
Density of blocks <sup>d,f</sup>	5.8	5.3	7.3	6.1	7.7	6.7
N.b. per block <sup>c</sup>	2.8	2.8	2.1	2.1	2.0	2.0
Density of branches <sup>c</sup>	16.1	14.5	15.6	13.0	15.4	13.2
A:B <sup>g</sup>	0.9:1	0.9:1	0.8:1	0.8:1	0.8:1	0.9:1
A:Ba <sup>g</sup>	1.4:1	1.4:1	1.2:1	1.2:1	1.5:1	1.4:1
Ba:Bb <sup>g</sup>	2.0:1	1.9:1	2.0:1	1.8:1	1.0:1	1.9:1
% B-chains as <sup>h</sup>						
B2	–	3	–	5	–	1
Int.	8	3	11	3	–	2
B1b	17	15	11	15	25	19
B1a(l)	25	27	23	28	25	28
B1a(s)	25	24	22	22	25	23
Maltotetraose	8	8	11	9	–	6
Maltotriose	17	20	22	18	25	21

<sup>a</sup> Theoretical values are calculated from the models in Figs. 7 and 8 and compared with experimental values.

<sup>b</sup> Number of chains obtained from Figs. 7 and 8.

<sup>c</sup> From Table 3.

<sup>d</sup> From Bertoft et al. (1999).

<sup>e</sup> The ratio of linear:branched building blocks, in which the branched blocks are eII–eVI.

<sup>f</sup> From Table 1.

<sup>g</sup> From Table 2.

<sup>h</sup> The proportion of different types of B-chains obtained by HPAEC-PAD.

part of the attacked chains, or if they preferentially were the residues of the other residual fragment, was uncertain. However, the reported common configuration of the Staudinger type with one D-glucosyl residue between two branches (Umeki & Yamamoto, 1975), should be seen as d.p.  $\geq 5$  in our experiments.

#### 4.3. Structure models of units from domains A and B

As was shown in our preceding report, the fractions of dextrans were structurally different on the basis of the distribution of building blocks obtained by an extensive alpha-amylolysis (Bertoft et al., 1999). Because of the regularity in the alpha-amylolysis pattern of the samples containing dextrans from DomA, they possibly originated from the more organized crystalline areas in the granules. The universal distance of one amorphous and one crystalline lamellae is close to 9 nm (Jenkins, Cameron & Donald, 1993). The length of the amorphous portion increases with increasing amylopectin content of the starch granule

(Jenkins & Donald, 1995). If assuming that waxy-maize starch granules are similar to waxy-rice, the width of the amorphous lamellae should be approximately 3 nm, whereas the crystalline lamellae is 6 nm (Jenkins & Donald, 1995).

A theoretical model for the structure of a fragment in DomA, including two clusters of the waxy-rice amylopectin, is shown in Fig. 7. The crystalline lamellae are build up of the external chains, mostly in double helical conformation, and scattered branches (Jane et al., 1997). It is known that each turn of a single helical strand comprises six D-glucosyl residues with a length of 2.1 nm in the direction of the helical axis (Imberty et al., 1991). The crystalline lamellae will thus contain chains with a maximum length of  $\sim 17$  residues and would include the A-chains and the shortest B-chains.

Very little is known about the conformation of the chains within the amorphous lamellae. Recent advances in molecular modelling suggest, however, that the chains behind the branches (at the reducing end-side of the branches) in this

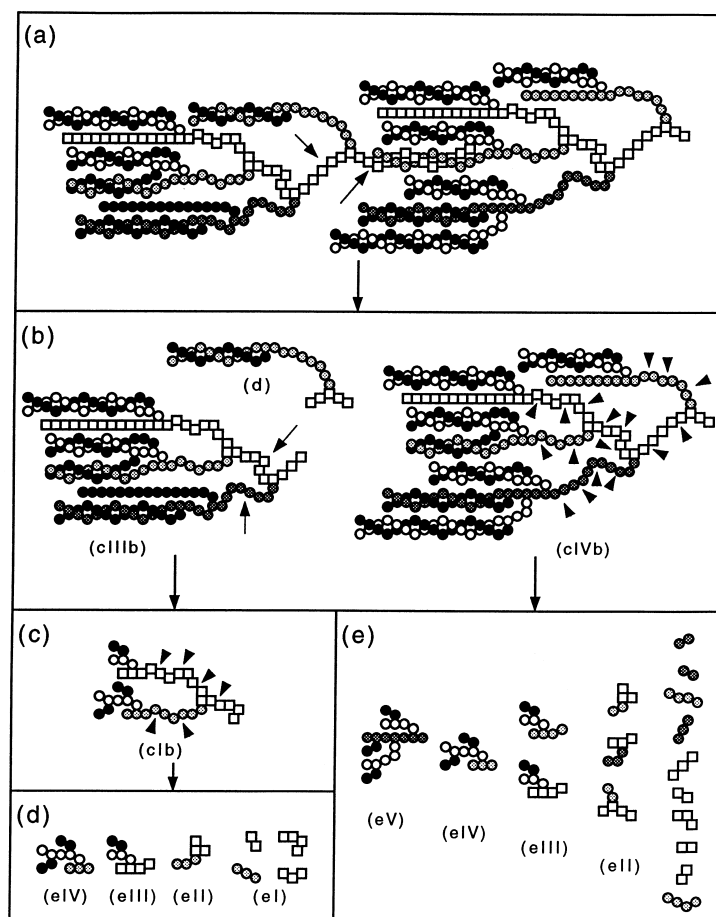


Fig. 8. Proposed model of the structure of domain B (DomB): (a) long chain segments between clusters within an amorphous “growth ring” are initially attacked by the alpha-amylolysis (arrows); (b) the attack results in  $\alpha$ -dextrins of different sizes, including very small ones (dextrin d); (c) a further hydrolysis (arrows) of dextrin cIIIb results in smaller fragments, that were isolated as  $\phi$ , $\beta$ -LD (dextrin cIb), and an extensive alpha-amylolysis attacks at longer internal chains within the cluster (small arrows); (d) branched building blocks (eII–eIV) and short linear maltodextrins (eI) are released; (e) the building blocks from larger fragments obtained at earlier stages of alpha-amylolysis (cIVb) results in a broader size-range of the building blocks: black circles represent A-chains, white circles B1a(s)-chains, light gray circles B1a(l)-chains, dark gray circles B1b-chains, and squares long chains (intermediate and B2-chains).

area considerably bend into directions perpendicular to that of the double helices (O’Sullivan & Pérez, 1999). This is schematically indicated in Fig. 7(a) and shows that the actual chain lengths within the amorphous area can be much longer than the width of 3 nm suggests. The irregular structure of the chains would also allow flexibility and permit them to rearrange into energetically more perfect conformations. Such movements appear to increase the perfection of the crystalline lamellae during annealing of starch granules (Tester, Debon & Karkalas, 1998).

The longest chain interconnects the two clusters (Hizukuri, 1986). This B2-chain is preferentially attacked by the alpha-amylase at a long internal chain segment, as indicated in Fig. 7(a). (In this case the right-handed part of the chain will be obtained as maltotriose after debranching of the residual limit dextrin.) The attack results in the production of intermediate dextrins representing single clusters. After the production of their  $\phi$ , $\beta$ -LD, they resemble the composition of sample 10.1 (Fig. 7(b)). One group of the dextrins in sample 10.1 was called cIVa (Bertoft et al., 1999). As was

shown in Fig. 4(a), the alpha-amylase attack resulted in the production of chains of intermediate lengths of d.p. 23–27. Similar chains were also typically produced from the amylopectins of waxy-maize (Bertoft, 1991b) and potato (Zhu & Bertoft, 1996). In the model, this chain is found preferentially within the amorphous lamellae, which would explain the existence of comparatively long chains within the clusters. B1b- and B1a(1)-chains also originate from the amorphous lamellae. The distances between the branch points in the lamellae are comparatively long with i.c.l. of 6–8. This will allow the alpha-amylase to slowly attack these segments during an extensive hydrolysis into the branched building blocks eII–eVI (Fig. 7(c)). A repetitive attack releases the very small linear fragments of d.p. 2–4 (eI). Thus, in the model the building blocks are scattered within the cluster through connections to the B-chains within the amorphous lamellae. The building blocks themselves are the major contributors to the crystalline lamellae. The smallest, single branched building blocks (eII), however, represent mainly the branches in the amorphous lamellae. As seen

in Table 4, the parameters of the model are within a reasonable agreement with the experimental values found for domain A in this and in our previous study (Bertoft et al., 1999).

The dextrins from domain B possessed more irregular structures and less of the larger building blocks. We suggested that they are found within the large amorphous rings of the granules (Bertoft et al., 1999). In Fig. 8(a) a model showing a part of this domain is drawn. The structure is less regular when compared to DomA (Fig. 7) and the chains are not organized into crystalline and amorphous lamellae. However, the same types of chains are found as in DomA. The alpha-amylase attacks initially at long internal chains giving dextrins of a range of sizes, of which the smallest (dextrin d in Fig. 8(b)) are similar to those isolated in sample 13. The dextrins contain increased amounts of the intermediate and the B1b-chains, as suggested in Fig. 4(b) and (c).

A further hydrolysis split off some building blocks from the irregular cluster-like structures (dextrin cIIIb), thereby slowly reducing the molecular weight (Bertoft et al., 1999). Finally, the residual fragments resemble those found in samples 11.1 and 11.2 (Fig. 8(c)). The building blocks in these fragments have intermediate sizes (Fig. 8(d)) and the proportion of the linear dextrins eI is higher than in the clusters of DomA (Table 4). Larger dextrins, as those found in samples 7.2.1 and 3 (dextrin cIVb in Fig. 8(b)), have a broader size-range of building blocks (Fig. 8(e)). The loose inner structure is rich in internal segments that can be attacked repetitively during an extensive alpha-amylolysis, giving a higher ratio of linear:branched blocks.

Several parameters of the structural models are compared with the experimental data in Table 4. Some of the parameters agree better than others. It is clear that the experimental data were obtained as an average of a large number of individual molecular structures in each sample, whereas the models suggest the major architectural features of the domains illustrated by single examples. Overall, the density of building blocks in the model of DomB is slightly higher than that of DomA. However, the number of branches per block is higher in DomA leading to a slightly higher average density of branches.

## Acknowledgements

We are grateful to Dr Serge Pérez for valuable comments on the manuscript. This work was supported by a grant from the Ellida and Tor Mauritz Ljungberg Foundation.

## References

Asaoka, M., Okuno, K., & Fuwa, H. (1985). Effect of environmental temperature at the milky stage on amylose content and fine structure of amylopectin of waxy and nonwaxy endosperm starches of rice (*Oryza sativa* L.). *Agricultural and Biological Chemistry*, 49, 373–379.

Atkin, N. J., Abeysekera, R. M., Cheng, S. L., & Robards, A. W. (1998). An experimentally-based predictive model for the separation of amylopectin subunits during starch gelatinization. *Carbohydrate Polymers*, 36, 173–192.

Baldwin, P. M., Adler, J., Davies, M. C., & Melia, C. D. (1998). High resolution imaging of starch granule surfaces by atomic force microscopy. *Journal of Cereal Science*, 27, 255–265.

Bertoft, E. (1989). Partial characterization of amylopectin alpha-dextrins. *Carbohydrate Research*, 189, 181–193.

Bertoft, E. (1991). Chains of intermediate lengths in waxy-maize amylopectin. *Carbohydrate Research*, 212, 245–251.

Bertoft, E. (1991). Investigation of the fine structure of alpha-dextrins derived from amylopectin and their relation to the structure of waxy-maize starch. *Carbohydrate Research*, 212, 229–244.

Bertoft, E., & Spoof, L. (1989). Fractional precipitation of amylopectin alpha-dextrins using methanol. *Carbohydrate Research*, 189, 169–180.

Bertoft, E., Zhu, Q., Andtfolk, H., & Jungner, M. (1999). Structural heterogeneity in waxy-rice starch. *Carbohydrate Polymers*, 38, 349–359.

Dubois, M., Gilles, K. A., Hamilton, J. K., Rebers, P. A., & Smith, F. (1956). Colorimetric method for determination of sugars and related substances. *Analytical Chemistry*, 28, 350–356.

Enevoldsen, B. S., & Juliano, B. O. (1988). Ratio of A chains to B chains in rice amylopectins. *Cereal Chemistry*, 65, 424–427.

Gallant, D. J., Bouchet, B., & Baldwin, P. M. (1997). Microscopy of starch: evidence of a new level of granule organization. *Carbohydrate Polymers*, 32, 177–191.

Hanashiro, I., Abe, J.-i., & Hizukuri, S. (1996). A periodic distribution of chain length of amylopectin as revealed by high-performance anion-exchange chromatography. *Carbohydrate Research*, 283, 151–159.

Hizukuri, S. (1986). Polymodal distribution of the chain lengths of amylopectins, and its significance. *Carbohydrate Research*, 147, 342–347.

Hizukuri, S., & Maehara, Y. (1990). Fine structure of wheat amylopectin: the mode of A to B chain binding. *Carbohydrate Research*, 206, 145–159.

Imberty, A., Buléon, A., Tran, V., & Pérez, S. (1991). Recent advances in knowledge of starch structure. *Starch/Stärke*, 43, 375–384.

Inouchi, N., Glover, D. V., & Fuwa, H. (1987). Chain length distribution of amylopectins of several single mutants and the normal counterpart, and sugary-1 phyto glycogen in maize (*Zea mays* L.). *Starch/Stärke*, 39, 259–266.

Jane, J. I., Wong, K.-s., & McPherson, A. E. (1997). Branch-structure difference in starches of A- and B-type X-ray patterns revealed by their Naegeli dextrins. *Carbohydrate Research*, 300, 219–227.

Jenkins, P. J., Cameron, R. E., & Donald, A. M. (1993). A universal feature in the structure of starch granules from different botanical sources. *Starch/Stärke*, 45, 417–420.

Jenkins, P. J., & Donald, A. M. (1995). The influence of amylose on starch granule structure. *International Journal of Biology of Macromolecules*, 17, 315–321.

Koch, K., Andersson, R., & Åman, P. (1998). Quantitative analysis of amylopectin unit chains by means of high-performance anion-exchange chromatography with pulsed amperometric detection. *Journal of Chromatography A*, 800, 199–206.

Ong, M. H., Jumel, K., Tokarczuk, P. F., Blanshard, J. M. V., & Harding, S. E. (1994). Simultaneous determinations of the molecular weight distributions of amyloses and the fine structures of amylopectins of native starches. *Carbohydrate Research*, 260, 99–117.

O'Sullivan, A. C., & Pérez, S. (1999). The relationship between internal chain length of amylopectin and crystallinity in starch. *Biopolymers*, in press.

Peat, S., Whelan, W. J., & Thomas, G. J. (1952). Evidence of multiple branching in waxy maize starch. *Journal of the Chemical Society*, 4546–4548.

Robyt, J., & French, D. (1963). Action pattern and specificity of an amylase from *Bacillus subtilis*. *Archives of Biochemistry and Biophysics*, 100, 451–467.

- Tester, R. F., Debon, S. J. J., & Karkalas, J. (1998). Annealing of wheat starch. *Journal of Cereal Science*, 28, 259–272.
- Umeki, K., & Yamamoto, T. (1975). Structures of multi-branched dextrins produced by saccharifying  $\alpha$ -amylase from starch. *Journal of Biochemistry*, 78, 897–903.
- Yamaguchi, M., Kainuma, K., & French, D. (1979). Electron microscopic observations of waxy maize starch. *Journal of Ultrastructure Research*, 69, 249–261.
- Yokobayashi, K., Misaka, A., & Harada, T. (1970). Purification and properties of *Pseudomonas isoamylase*. *Biochimica Biophysica Acta*, 212, 458–469.
- Yun, S. H., & Matheson, N. K. (1993). Structures of the amylopectins of waxy, normal, amylose-extender, and wx:ae genotypes and of the phytoglycogen of maize. *Carbohydrate Research*, 243, 307–321.
- Zhu, Q., & Bertoft, E. (1996). Composition and structural analysis of alpha-dextrins from potato amylopectin. *Carbohydrate Research*, 288, 155–174.